SUPPLEMENT TO THE *WELDING JOURNAL*, AUGUST 2013
Sponsored by the American Welding Society and the Welding Research Council

Microstructure and Wear Properties of Fe-2 wt-% Cr-X wt-% W-0.67 wt-% C Hardfacing Layer

Electrodes with different additions of tungsten were evaluated to determine the effect on hardness and wear resistance

BY J. YANG, Y. YANG, Y. ZHOU, X. QI, Y. GAO, X. REN, AND Q. YANG

ABSTRACT

Electrodes with different W additives for hardfacing the workpieces of high-carbon alloy steel were developed. The microstructure was observed by optical microscopy and field emission scanning electron microscope equipped with energy-dispersive X-ray spectrometry. The phase structure was determined by X-ray diffraction. The hardness and wear resistance, respectively, of the hardfacing surface layer were measured. The relative curve between mass fraction of each phase and temperature was calculated by *Thermo-Calc*. The results show that, the microstructure of the hardfacing surface layer without W additive consists of α-Fe, γ-Fe, M_7C_3, and $M_{23}C_6$ carbides. However, MC carbide initiates in the hardfacing surface layer and its amount increases with the increase of W additive, while that of M_7C_3 decreases. With the increase of W additive, the hardness and wear resistance of the hardfacing surface layer both increase, and they are the largest when the W additive is 4 wt-%. The C content of the martensite matrix decreases gradually with the increase of W additive. Moreover, only elements C and W exist in MC carbide. With the increase of W content in the hardfacing surface layer, the starting precipitation temperature and the largest mass fraction of MC both increase. However, those of M_7C_3 both decrease.

Introduction

Workpieces manufactured with high-carbon alloy steel, such as roller and die components, are widely applied in industrial production (Refs. 1–3). After being in service for a period of time, the workpieces fail because of excessive wear (Refs. 4, 5). The shape and size of the failed workpieces can be restored by means of remanufacturing technologies, in which hardface welding (hardfacing) is one of the most effective methods (Refs. 6–9).

Development of high-carbon alloy steel is characterized by the increase of Cr content so as to improve the strength and hardenability of the steel (Ref. 10). In recent years, in order to improve its wear resistance, alloy elements W and Mo were added (Refs. 11–13).

However, related research indicated that because of the high C content, cracks usually initiate on the surface of the workpieces manufactured with the high-carbon alloy steel after hardfacing, even if they were preheated and reheated after hardfacing (Ref. 8). So, the wide application of hardfacing technology for restoring and remanufacturing the high-carbon alloy steel workpieces is restricted. Moreover, the effects of alloy elements W and Mo are seldom reported.

Therefore, on the basis of research into the microstructure of medium carbon steel (Ref. 14), medium-high carbon steel (Refs. 15, 16), and high-chromium cast iron (Refs. 17, 18), a novel electrode was developed, by which no cracking occurred on the surface of the workpieces when they were preheated and reheated after hardfacing. Subsequently, the effect of W additive on the microstructure and wear resistance of the high-carbon steel hardfacing surface layer was researched, and the corresponding mechanism was analyzed, which can supply a theoretical foundation for improving the wear resistance of the hardfacing surface layer of high-carbon steel.

J. YANG, Y. YANG, Y. ZHOU, X. QI, and Q. YANG (qxyang@ysu.edu.cn) *are with State Key Laboratory of Metastable Materials Science and Technology, College of Materials Science and Engineering, Yanshan University, Qinhuangdao, China. Y. GAO is with School of Material Science and Engineering, Tongji University, Shanghai, China. X. REN is with School of Engineering, Liverpool John Moores University, Liverpool, UK.*

KEYWORDS

Fe-Cr-W-C Alloy
Hardfacing
Microstructure
Wear Resistance
Carbides

Experimental Procedure

Experimental Materials

An electrode for hardfacing high-carbon steel was manufactured. The core of the electrode was made of H08A low-carbon steel, whose composition is listed in Table 1. The outer coating was composed of ferrosilicon, ferrochrome, ferromanganese, and ferrotungsten (W additive). In order to analyze the effect of W additive on microstructure and property of the hardfacing surface layer, the mass fractions of the ferrotungsten added into the outer coating were 0, 2, 4, and 6 wt-%, respectively.

Experimental Methods

Base metals for the welding surface were prepared from Q235 low-carbon steel plates, and three layers were welded onto each specimen. The process was shielded metal arc welding (SMAW). A schematic diagram of the welding pattern and welding parameters used in this work appear in Fig. 1 and Table 2, respectively.

In order to analyze the effect of the W additive on the properties of the hardfacing surface layer, its macrohardness was measured using a HR-105A Rockwell hardness tester with a load of 150 kg for

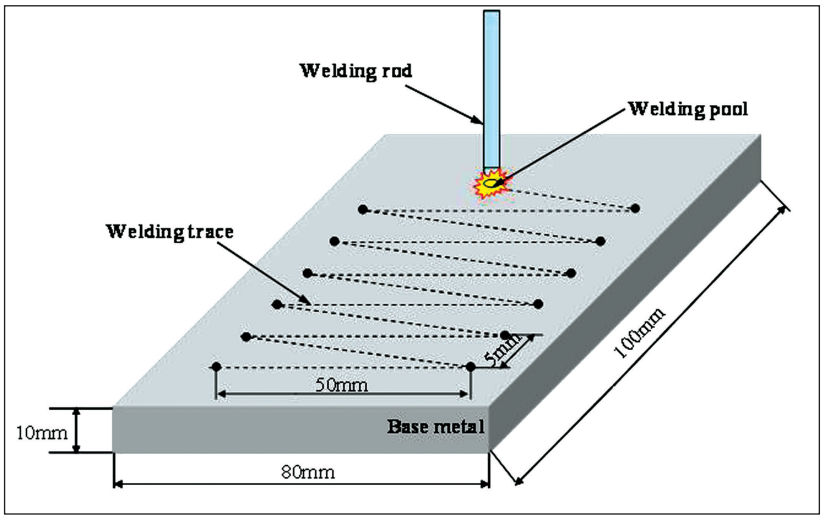

Fig. 1 — Welding technology schematic diagram.

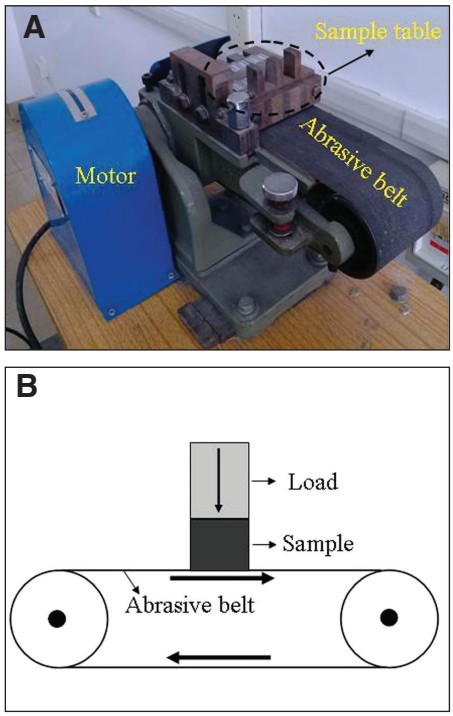

Fig. 2 — The abrasive belt-type wear testing machine. A — Photograph; B — schematic.

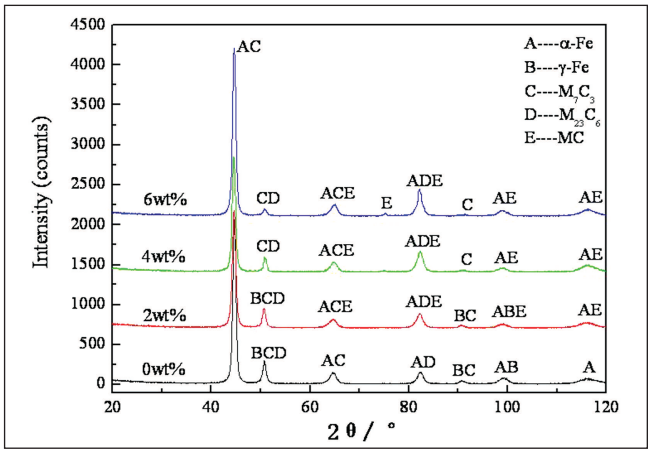

Fig. 3 — XRD patterns of the hardfacing surface layers with different W additives.

10 s. Subsequently, a wear resistance test was carried out on an abrasive belt-type wear testing machine, in which SiC of 80 mesh was selected as the abrasive material and the wear velocity of the abrasive belt was 1.8×10^4 mm · min^{-1}. The abrasive belt wear testing machine and a schematic diagram are shown in Fig. 2. An electronic balance with an accuracy of 0.1 mg was used to weigh the mass loss of the layer per 30 min. After the wear test, the worn surface morphology was observed by scanning electron microscope (SEM) of type KYKY-2800.

The microstructure of the hardfacing surface layer, which was etched with 4% nitric acid alcohol after being metallographically polished, was characterized by an Axiovert 200 MAT optical microscope (OM) and a Hitachi S4800 field emission scanning electron microscope (FESEM) equipped with energy-dispersive X-ray spectrometry (EDS). The phase structure was determined by X-ray diffraction (XRD) of type D/max-2500/PC. The relative curve between mass fraction of each phase and temperature was calculated by thermodynamics software *Thermo-Calc.*

Experimental Results

Influence of W Additive on the Phase-Structure of the Hardfacing Surface Layer

Figure 3 illustrates XRD analysis results of the hardfacing surface layers with different W additives. As shown, without the W additive, the phase microstructure consists of α-Fe, γ-Fe, $M_{23}C_6$, and M_7C_3 carbides. When the W additive is 2 wt-%, besides α-Fe, γ-Fe, $M_{23}C_6$, and M_7C_3 carbides, MC carbide initiates in the hardfacing surface layer. By quantitative analysis, the content of retained austenite decreases from 15.8 to 6.4%. When the W additive is 4 wt-%, the γ-Fe disappears absolutely. Meanwhile, the amount of M_7C_3 decreases and that of MC increases. With 6 wt-% W additive, the amount of M_7C_3 decreases and that of MC increases continually in the hardfacing surface layer.

Influence of W Additive on the Microstructure of the Hardfacing Surface Layer

The microstructures of the hardfacing surface layers with different W additives are shown in Fig. 4. Without W additive, the microstructure consists of black needle martensite (normal martensite) and white reticular martensite (high-C alloy martensite), in which the latter with high-carbon content and alloy elements precipitate on the crystal boundary. When the W additive is 2 wt-%, the high-carbon alloy martensite becomes intermittent. With

Table 1 — Chemical Composition of H08A (wt-%)

Element	C	Mn	Si	Cr	Ni	S	P
Content	≤0.10	0.30–0.50	≤0.03	≤0.2	≤0.03	≤0.03	≤0.03

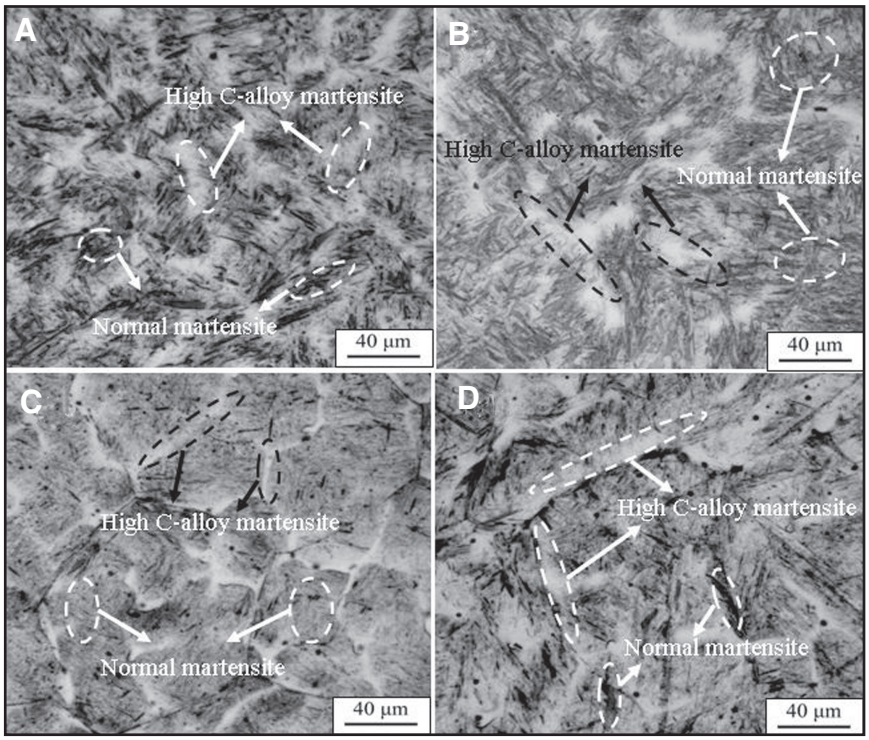

Fig. 4 — Microstructures of the hardfacing surface layers with different W additives. A — 0 wt-%; B — 2 wt-%; C — 4 wt-%; D — 6 wt-%.

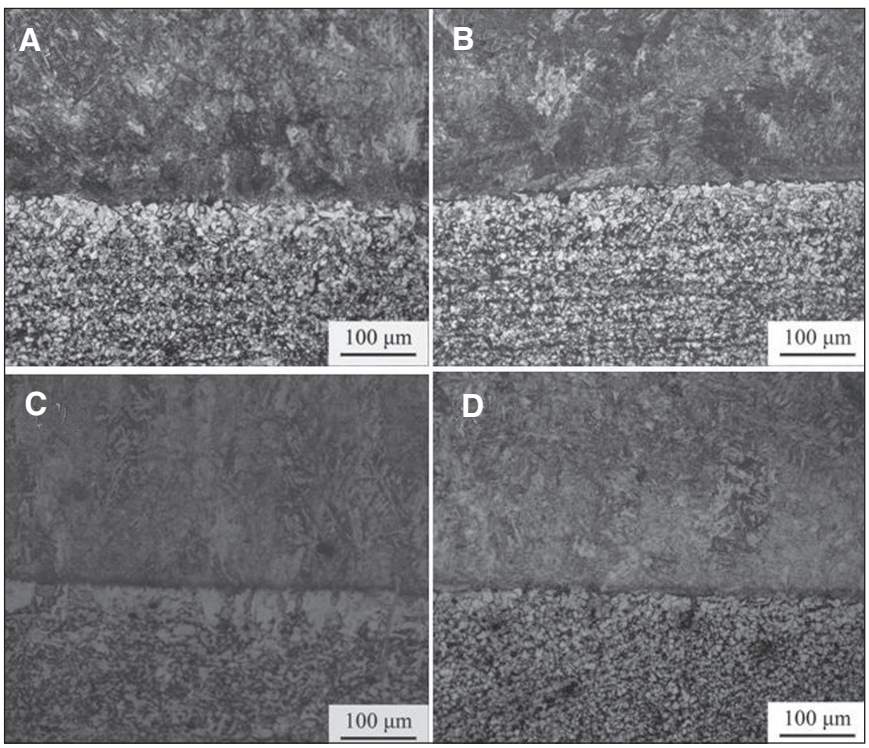

Fig. 5 — Vertical morphologies of the hardfacing surface layers with different W additives. A — 0 wt%; B — 2 wt-%; C — 4 wt-%; D — 6 wt-%.

Table 2 — Welding Parameters

Welding Current	Welding Voltage	Welding Speed	Overlap of Welding Tracks
140–150 A	24–26 V	1.1–1.7 mm/s	50%

4 wt-% W additive, the high-C alloy martensite refines obviously. When the W additive is 6 wt-%, the high-C alloy martensite further refines and dissolves in the matrix.

Figure 5 indicates the vertical morphologies of the hardfacing surface layers with different W additives. From it, because of the favorable welding process, binding modes between the matrix metal and the hardfacing metal with different W additives are all the typical metallurgical ones. The effect of W additives on the weldability is inconspicuous.

Influence of W Additive on the Hardness of the Hardfacing Surface Layer

The hardness of the hardfacing surface layers with different W additives are shown in Fig. 6. The hardness without W additive is 61.5 HRC. With the increase of W additive, the hardness increases gradually. When the W additive is 4 wt-%, the hardness is the largest at 66.0 HRC. With further increase of W, the hardness decreases instead, and it is 64.9 HRC with 6 wt-% W additive.

Influence of W Additive on the Wear Resistance of the Hardfacing Surface Layer

The wear loss curves of the hardfacing surface layers with different W additives are shown in Fig. 7. As shown, the weight loss of the hardfacing surface layer without W additive is the largest. With 2 wt-% W additive, the wear resistance improves significantly and there is an obvious reduction in wear weight loss. When the W additive reaches 4 wt-%, wear resistance of the hardfacing surface layer is the highest. However, with further increase of W, the wear weight loss increases sharply.

Figure 8 illustrates the wear morphologies of the hardfacing surface layers with different W additives. As seen in Fig. 8A, without W additive, surface scratches are both wide and deep. With the increase of W, surface scratches are shallow and narrow. When the W is 4 wt-%, the scratches are the shallowest, as shown in Fig. 8C. With further increase of W, surface scratches are deep and broad, as shown in Fig. 8D.

Wear Resistance-Enhanced Mechanism of the Hardfacing Layer with W Additive

Characteristics on MC Carbide in the Hardfacing Surface Layer

From the above results, with the increase of W, the wear resistance of the hardfacing surface layer increases. Meanwhile, the amount of MC carbide increases while that of high-carbon alloy martensite

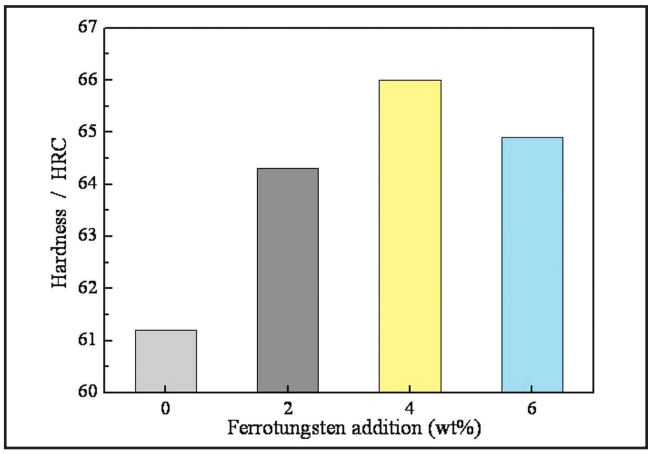

Fig. 6 — Hardness of surface layer with different W additives.

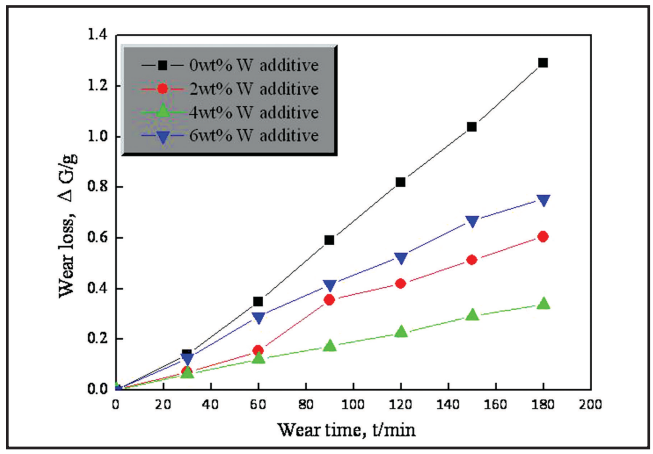

Fig. 7 — Wear loss of the hardfacing surface layer with different W additives.

decreases. So the wear resistance is related closely with MC carbide and high-carbon alloy martensite. Therefore, the MC carbide and high-carbon alloy martensite with different W additives were investigated in this work.

Figure 9 illustrates FESEM of the hardfacing surface layers with different W additives. With the increase of W, the strip high-carbon alloy martensite, which distributes on the crystal boundary, refines gradually, and nearly disappears completely when the W additive is 6 wt-%. Meanwhile, with the increase of W, a few small granular particles appear in the hardfacing surface layer.

Figure 10 is the line energy spectrum of the granular particle in the hardfacing surface layer with the 2 wt-% W. Combined with Fig. 3, it can be inferred that the granular particle is MC carbide.

Influence of W additive on the Carbides of the Hardfacing Surface Layer

In order to analyze the influence of W additive on the carbides of the hardfacing surface layers during welding solidification process, the hardfacing surface layers with four W additives were taken and their chemical compositions are listed in Table 3.

The relation curves between mole fractions of alloy elements and temperature in MC, M_7C_3, and $M_{23}C_6$ carbides, which were calculated by *Thermo-Calc* software, and are shown in Fig. 11. From Fig. 11A, it can be seen that only C and W exist in the MC carbide. While in the M_7C_3 and $M_{23}C_6$ carbides, there is mainly Fe and Cr, which are shown in Fig.11B and C. It illustrates that the W content mainly affects the MC carbide instead of M_7C_3 and $M_{23}C_6$ carbides.

The curves between mass fraction of each phase and temperature in the hardfacing surface layers with different W contents are shown in Fig. 12. Without W content, no MC carbide precipitates from the hardfacing surface layer. With the increase of W content, MC carbide initiates gradually, and the beginning precipitation temperature of MC carbide change is not obvious. However, the maximum amount of MC carbide clearly increases 4.2% when the W content is 1.74 wt-%. Meanwhile, the beginning precipitation temperature of M_7C_3 decreases from 778° to 695°C and the maximum amount decreases from 9.4 to 6.3 wt-%.

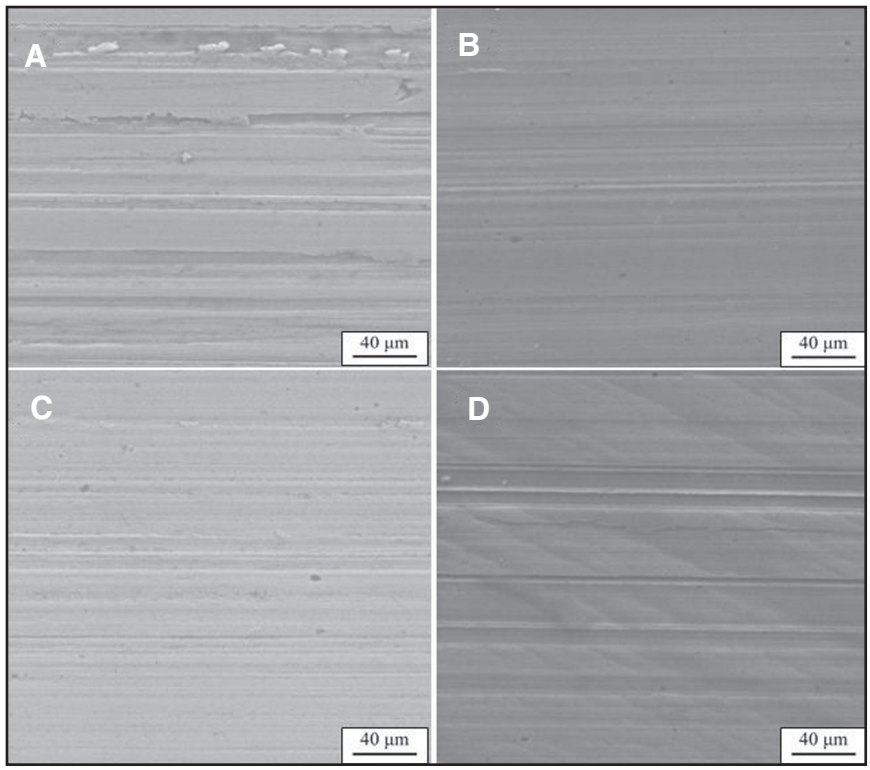

Fig. 8 — Wear morphologies of the hardfacing surface layer with different W additives. A — 0 wt-%; B — 2 wt-%; C — 4 wt-%; D — 6 wt-%.

Table 3 — Chemical Compositions of the Hardfacing Surface Layers (wt-%)

C	Cr	W	Si	Mn	Fe
0.67	2.05	0	0.614	0.565	Bal
0.67	2.05	0.58	0.614	0.565	Bal
0.67	2.05	1.46	0.614	0.565	Bal
0.67	2.05	1.74	0.614	0.565	Bal

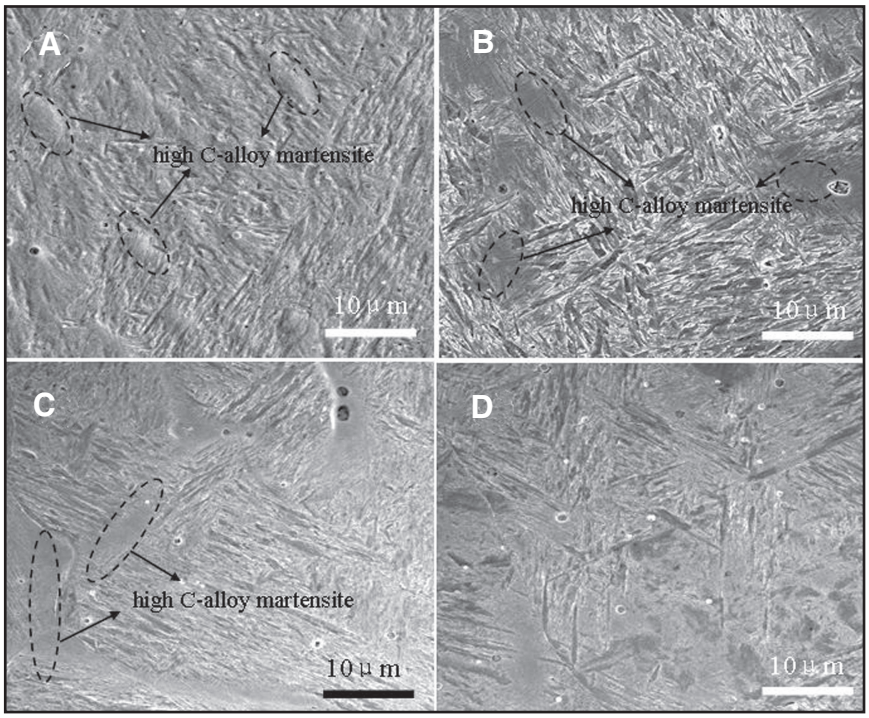

Fig. 9 — FESEM of the hardfacing surface layers with different W additives. A — 0 wt-%; B — 2 wt%; C — 4 wt-%; D — 6 wt-%.

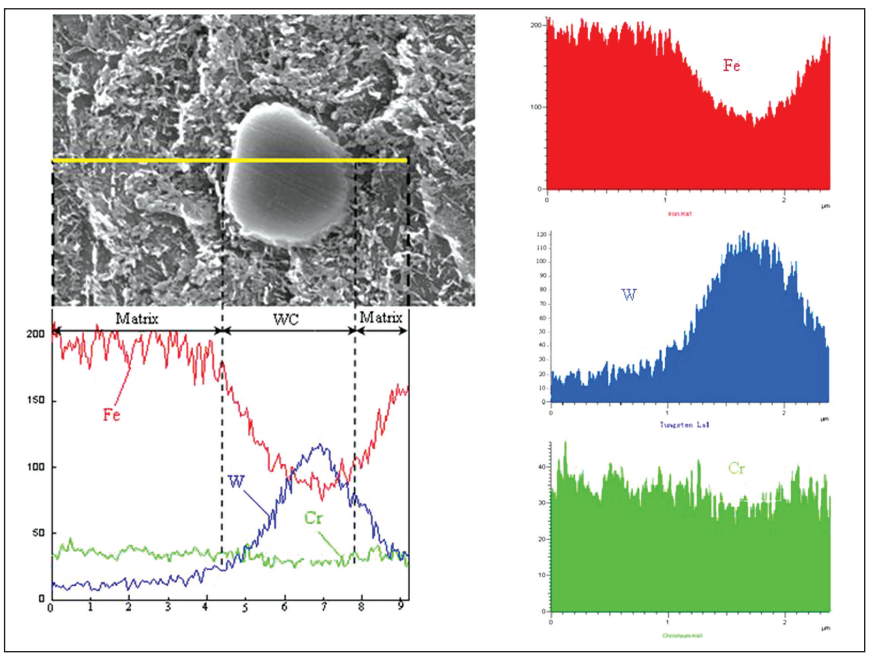

Fig. 10 — Line energy spectrum of the granular particle in the hardfacing surface layer.

Table 4 — EDS of the Martensite in the Hardfacing Surface Layers with Different W Additives (wt-%)

W Additive	C	Si	Cr	Mn	Fe	W
0 wt-%	3.76	0.89	2.30	0.69	92.36	—
2 wt-%	3.57	0.89	2.03	0.71	91.84	0.96
4 wt-%	3.04	1.01	2.49	0.76	91.40	1.29
6 wt-%	2.73	0.72	2.15	0.57	91.13	2.79

Influence of W Additive on the Martensite of the Hardfacing Surface Layer

Energy-dispersive spectroscopy (EDS) results of the martensite in the hardfacing surface layers with different W additives are listed in Table 4. With the increase of W additive, the C content in the martensite of the hardfacing surface layer decreases gradually, from 3.76 to 2.73 wt-%. The reason is that, with the W increases, the amount of MC carbide increases, so the C content in the martensite is reduced.

As previously mentioned, with the increase of W, the amount of MC carbide clearly increases while the content of C in the martensite decreases gradually. Therefore, the wear resistance change tendency of the hardfacing surface layer with different W additives can be explained as follows:

The amount of MC carbide, which can be the wear-resisting phase (Refs. 19, 20) of the hardfacing surface layer, increases with the increase of W. Without W, the microstructure is mainly martensite without MC carbide, so the weight loss of the hardfacing surface layer is largest during the wear process. With the increase of W, MC carbide initiates in the hardfacing surface layer and hard wear-resistant phase increases, so its weight loss decreases. When the W additive is 4%, MC carbide exists largely in the hardfacing surface layer, and its wear resistance is the greatest. With a further increase of W to 6 wt-%, although the amount of MC carbide increases continually, the C content in martensite matrix decreases, which cannot support the wear-resisting phase of MC carbide favorably, so the wear resistance of the hardfacing surface layer decreases again.

Conclusions

1) The microstructure of the hardfacing surface layer without W additive consists of α-Fe, γ-Fe, M_7C_3, and $M_{23}C_6$ carbides. With the increase of W additive, MC carbide initiates gradually, and the amount of MC increases while that of M_7C_3 and γ-Fe decreases.

2) Hardness and wear resistance of the hardfacing surface layers both increase with the increase of W additive, which are greatest when W additive is 4 wt-%.

3) Only the elements C and W exist in MC carbide. With the increase of W content in the hardfacing surface layer, the starting precipitation temperature and the mass fraction maximum of MC both increase. However, those of M_7C_3 both decrease.

4) With the increase of W additive, the C content in the martensite of the hardfacing surface layer decreases gradually, from 3.76 to 2.73 wt-%.

References

1. Ashok, K. S., and Karabi, D. 2008. Microstructure and abrasive wear study of (Ti,W) C-reinforced high-manganese austenitic steel matrix composite. *Materials Letters* 62(24): 3947–3950.

2. Dennis, W. H., and William, V. G. 2008. Crystallography and metallography of carbides in high-alloy steels. *Materials Characterization* 59(7): 825–841.

3. Khodir, S. A., Morisada. Y., Ueji. R., and Fujii, H. 2012. Microstructures and mechanical properties evolution during friction stir welding of SK4 high-carbon steel alloy. *Materials Science and Engineering* A 558(15): 572–578.

4. Pellizzari, M., Molinari, A., and Straffelini, G. 2005. Tribological behaviour of hot rolling rolls. *Wear* 259(7–12): 1281–1289.

5. Yang, K., Yu, S. F., Li, Y. B., and Li, C. J. 2008. Effect of carbonitride precipitates on the abrasive wear behaviour of hardfacing alloy. *Applied Surface Science* 254(16): 5023–5027.

6. Zhou, Y. F., Yang, Y. L., Yang, J., Hao, F. F., Li, D., Ren, X. J., and Yang, Q. X. 2012. Effect of Ti additive on $(Cr, Fe)_7C_3$ carbide in arc surfacing layer and its refined mechanism. *Applied Surface Science* 258(17): 6653–6659.

7. Mirjana, F., and Endre, R. 2011. Strain hardening of austenite in Fe–Cr–C–V alloys under repeated impact. *Wear* 270(11-12): 800–805.

8. NAVA, J. C. 2009. Cost-effective thermal spray coatings for the boiler industry. *Welding Journal* 88(7): 38–41.

9. Buchanan, V. E., McCartney, D. G., and Shipway, P. H. 2008. A comparison of the abrasive wear behaviour of iron-chromium based hardfaced coatings deposited by SMAW and electric arc spraying. *Wear* 264(7-8): 542–549.

10. Ghaziof, S., Raeissi, K., and Golozar, M. A. 2010. Improving the corrosion performance of Cr–C amorphous coatings on steel substrate by modifying the steel surface preparation. *Surface and Coatings Technology* 205(7): 2174–2183.

11. Zhang, B. S., Yi, Y. J., Zhang, W., Liang, C. H., and Su, D. S. 2011. Electron microscopy investigation of the microstructure of unsupported Ni–Mo–W sulfide. *Materials Characterization* 62(7): 684–690.

12. Ivanova, G. V., Shchegoleva, N. N., Serikov, V. V., Kleinerman, N. M., and Belozerov. E. V. 2011. Structure of a W-enriched phase in Fe–Co–Cr–W–Ga alloys. *Journal of Alloys and Compounds* 509(5): 1809–1814.

13. Fu, X. L., Ge, H. L., Xing, Q. K., and Peng, Z. J. 2011. Effect of W ion doping on magnetic and dielectric properties of Ni–Zn ferrites by "one-step synthesis." *Materials Science and Engineering* B 176(12): 926–931.

14. Ramana, P. V., Reddy, G. M., Mohandas, T., and Gupta, A. V. S. S. K. S. 2010. Microstructure and residual stress distribution of similar and dissimilar electron beam welds — Maraging steel to medium alloy medium carbon steel. *Materials & Design* 31(2): 749–760.

15. Oh, Y. S., Son, I. H., Jung, K. H., Kim, D. K., Lee, D. L., and Im, Y. T. 2011. Effect of initial microstructure on mechanical properties in warm caliber rolling of high-carbon steel. *Materials Science and Engineering:* A 528(18): 5833–5839.

16. Nayak, S. S., Anumolu, R., Misra, R. D. K., Kim, K. H., and Lee, D. L. 2008. Microstructure–hardness relationship in quenched and partitioned medium-carbon and high-carbon steels containing silicon. *Materials Science and Engineering* A 498(1-2): 442–456.

17. Menon, R., and Wallin, J. 2008. Specialty cored wires for wear and corrosion applications. *Welding Journal* 87(2): 31–36.

18. Menon, R. 2002. Recent advances in cored wires for hardfacing. *Welding Journal* 81(11): 53–58.

19. Niu, L. B., Xu, Y. H., and Wang, X. G. 2010. Fabrication of WC/Fe composite coating by centrifugal casting plus in-situ synthesis techniques. *Surface and Coatings Technology* 205(2): 551–556.

20. Tong, X., Li, F. H., Kuang, M., Ma, W. Y., Chen, X. H., and Liu, M. 2012. Effects of WC particle size on the wear resistance of laser surface alloyed medium-carbon steel. *Applied Surface Science* 258(7): 3214–3220.

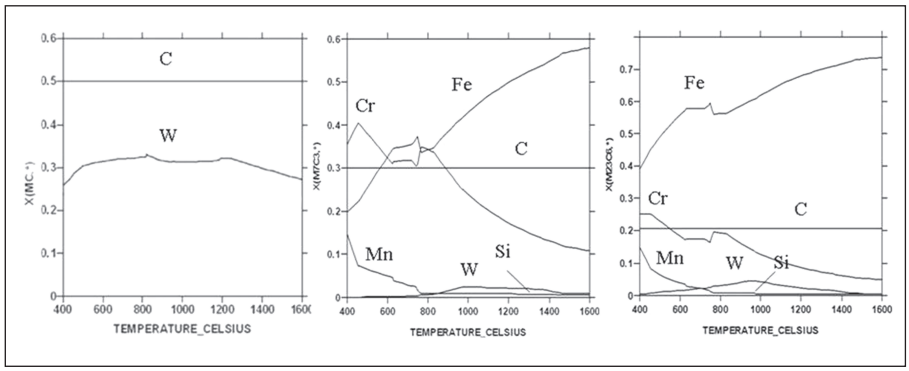

Fig. 11 — Relation curves between mole fractions of alloy elements and temperature. A — MC; B — M_7C_3; C — $M_{23}C_6$ carbides.

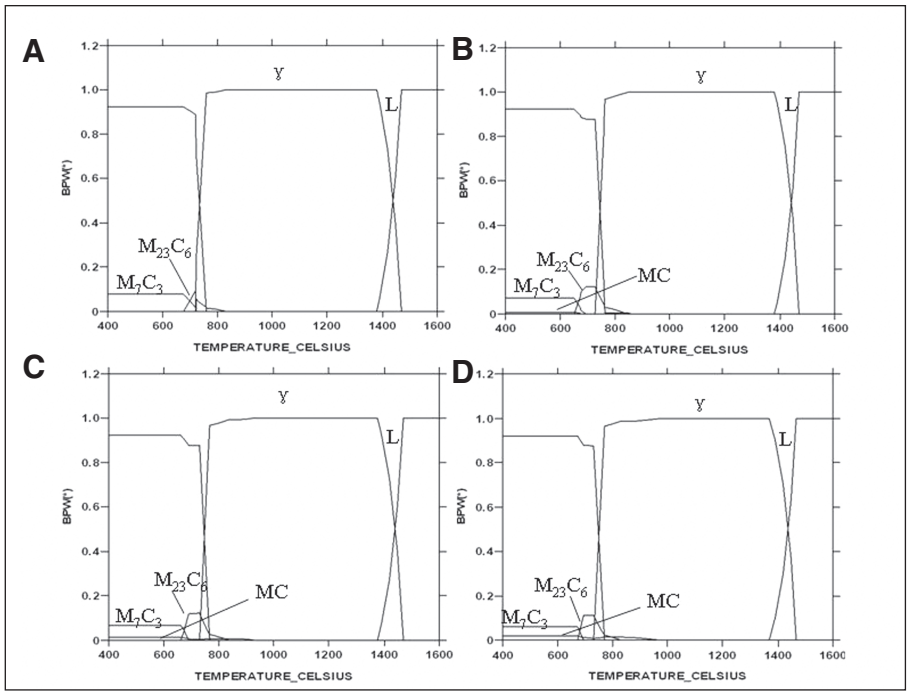

Fig. 12 — Curves between mass fraction of each phase and temperature in the hardfacing surface layers with different W contents. A — 0 wt-%; B — 2 wt-%; C — 4 wt-%; D — 6 wt-%.